

## Analysis of effective properties of materials by using the boundary element method

P. FEDELIŃSKI, R. GÓRSKI, T. CZYŻ,  
G. DZIATKIEWICZ, J. PTASZNY

*Institute of Computational Mechanics and Engineering  
Silesian University of Technology  
Konarskiego 18A  
44-100 Gliwice, Poland  
e-mail: Piotr.Fedelinski@polsl.pl*

IN THIS WORK DIFFERENT FORMULATIONS of the boundary element method (BEM) in an analysis of materials with inclusions are presented. Models of composites in the form of linear-elastic solids containing rigid inclusions, elasto-plastic composites and piezomagnetic composites are considered. It is assumed that perfectly bonded matrix and inclusions are made of homogeneous materials. The developed computer codes are used to compute effective material properties by considering unit cells or representative volume elements (RVE). The influence of volume fractions of inclusions on overall properties of materials is studied.

**Key words:** boundary element method, composites, effective material properties, representative volume element, unit cell.

Copyright © 2014 by IPPT PAN

### 1. Introduction

THE MACROSCOPIC BEHAVIOR OF MATERIALS depends on shape, size, distribution and properties of constituents at the microscopic level [1]. Performing experimental measurements on different material samples having various geometrical and mechanical properties is a hard task. Hence, there is a need for modeling methods which provide relations between properties at micro and macro level. The overall properties can be determined by experimental, analytical and computational methods. Analytical methods are limited to simple microstructures and small density of heterogeneities [1–4]. Among the computational methods the most popular methods are: the finite element method (FEM), the boundary element method (BEM), the finite difference method (FDM) and meshless methods (MM).

KAMIŃSKI [5] presented the boundary element method homogenisation of periodic linear elastic composites. DONG [6] has presented the integral equation formulations for single-domain and sub-domain models of a 2D infinite elastic medium containing inclusions, rigid lines and cracks. He compared the BEM

results of stresses and stress intensity factors for both models and revealed an excellent agreement of the solutions. LIU *et al.* [7, 8] analysed composites numerically using a 3D rigid-inclusion model and the fast multipole BEM. They have studied a single rigid sphere or multiple rigid fibres in a matrix, which were modelled as inner holes in an elastic medium. The results for displacements and stresses were in agreement with an analytical solution for a rigid sphere.

GHOSH and MOORTHY [9] developed a Voronoi cell finite element method (VCFEM) to analyse small deformation of elasto-plastic arbitrary heterogeneous two-dimensional microstructures. Numerical results were compared with analytical solutions. The influence of shape, size, orientation and distribution of inclusions on micro- and macroscopic responses was investigated. LEE and GHOSH [10] proposed two-scale analysis using the asymptotic homogenisation method and the VCFEM for analysis of microstructures of porous and composite materials. The orthotropic elasticity tensor was obtained by analysing microstructural problem with periodic boundary conditions. Parameters, which characterise plastic behaviour of the material, were determined from microstructural RVE analyses with asymptotic homogenisation. The results of the macroscopic analysis were compared with two-scale analysis with homogenisation.

A finite element analysis and micromechanics based averaging of a representative volume elements were performed by LEE *et al.* [11] to determine the effective properties of the three-phase electro-magneto-elastic composite. The influence of the phase volume fractions, the fibre arrangements in the RVE and the fibre material properties was taken into account. QIN [12] used a micromechanical boundary element algorithm to predict the effective properties of a piezoelectric material with defects such as cracks or holes. The self-consistent and Mori–Tanaka micromechanical methods were considered. Similarly, QIN [13] discussed applications of the boundary element method to piezoelectric composites in conjunction with homogenisation scheme for determining their overall properties. The considered composites consisted of inclusion and matrix phases and the model of the RVE was applied. Wang *et al.* [14] determined numerically the effective properties of voided piezoelectric materials using the boundary node method, which is a type of boundary-only meshless method. The transversely isotropic materials containing randomly distributed voids were considered. The two-dimensional analysis was performed with the RVE model and the material constants were obtained by imposing the appropriate boundary conditions.

An overview of formulations and applications of the boundary element method in modelling of various materials was presented by FEDELIŃSKI *et al.* in [15] and [16]. The same group of researchers applied the above mentioned method to analysis of composites containing large number of deformable in-

clusions [17], deformable fibres [18], rigid fibres [19], cracks [20] and piezocomposites [21]. In this work, the BEM formulations and numerical examples are given for solids containing rigid inclusions, elasto-plastic and piezoelectromagnetic composites. The influence of volume fraction of inclusions on effective properties is studied.

## 2. Materials with rigid inclusions

A body made of a homogeneous, isotropic and linear elastic material is considered, as shown in Fig. 1.

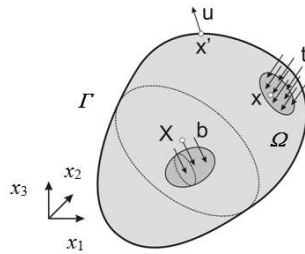


FIG. 1. Loading and displacements of an elastic body.

The external boundary of the body and its domain are denoted by  $\Gamma$  and  $\Omega$ , respectively. The body is statically loaded along the boundary  $\Gamma$  by boundary tractions  $t_j$  and inside the domain  $\Omega$  by body forces  $b_j$ . Displacements of the body are denoted by  $u_j$ . The points  $\mathbf{x}'$ ,  $\mathbf{x}$  and  $\mathbf{X}$  in Fig. 1 are a collocation point, the point on the external boundary  $\Gamma$  and inside the domain  $\Omega$ , respectively.

The relation between the loading of the body and its displacements can be expressed by the boundary integral equation – the Somigliana identity – in the form:

$$(2.1) \quad c_{ij}u_j(\mathbf{x}') + \int_{\Gamma} T_{ij}(\mathbf{x}', \mathbf{x})u_j(\mathbf{x})d\Gamma(\mathbf{x}) \\ = \int_{\Gamma} U_{ij}(\mathbf{x}', \mathbf{x})t_j(\mathbf{x})d\Gamma(\mathbf{x}) + \int_{\Omega} U_{ij}(\mathbf{x}', \mathbf{X})b_j(\mathbf{X})d\Omega(\mathbf{X}),$$

where  $c_{ij}$  is a constant, which depends on the position of the point  $\mathbf{x}'$ ,  $U_{ij}$  and  $T_{ij}$  are the Kelvin fundamental solutions of elastostatics. In equations the Einstein summation convention is used.

Assume that there are  $N$  rigid surfaces inside the body. The resultant structure presents a model of a composite material, where the body and the rigid surfaces play the role of a matrix and perfectly rigid flake-like inclusions, respectively.

The size, shape and orientation of the inclusions are arbitrary. In the present formulation the inclusions within the matrix are perfectly bonded to it and they are very thin.

When the reinforced body is loaded, interaction forces between the matrix and inclusions occur. They are treated as particular body forces acting along the surfaces of the inclusions, i.e., along the  $\Gamma_n$  surfaces ( $n = 1, 2, \dots, N$ ). In this case, the relation (2.1) can be written in the following form [19]:

$$(2.2) \quad c_{ij}(\mathbf{x}')u_j(\mathbf{x}') + \int_{\Gamma} T_{ij}(\mathbf{x}', \mathbf{x})u_j(\mathbf{x}) d\Gamma(\mathbf{x}) \\ = \int_{\Gamma} U_{ij}(\mathbf{x}', \mathbf{x})t_j(\mathbf{x})d\Gamma(\mathbf{x}) + \sum_{n=1}^N \int_{\Gamma_n} U_{ij}(\mathbf{x}', \mathbf{X})t_j^n(\mathbf{X}) d\Gamma_n(\mathbf{X}),$$

where  $t_j^n$  are interaction forces (surface boundary tractions) between the matrix and the rigid inclusions. Although the formulation for rigid inclusions is simpler and more efficient than for elastic inclusions, it requires additional considerations when dealing with rigid inclusions.

Because the inclusions are rigid, they are subjected to rigid-body motions. Thus, for a three-dimensional problem there are six unknowns for each inclusion, i.e., three translations and three rotations. Displacements  $u^n(X)$  at any point  $\mathbf{X}$  on an arbitrary inclusion  $n$  can be described by the rigid-body motions [7]:

$$(2.3) \quad \mathbf{u}^n(\mathbf{X}) = \mathbf{d} + \mathbf{w} \times \mathbf{p}(\mathbf{X}),$$

where  $\mathbf{d}$  is a rigid-body translational displacement vector,  $\mathbf{w}$  is a rotation vector,  $\mathbf{p}$  is a position vector for the point  $\mathbf{X}$  measured from a reference point (for example, a corner or the centre of an inclusion).

The considered body is in equilibrium, therefore the corresponding equilibrium equations of forces and moments are used. For a single rigid inclusion  $n$ , the expressions representing the equilibrium of forces and equilibrium of moments have the following form:

$$(2.4) \quad \int_{\Gamma_n} \mathbf{t}^n(\mathbf{X})d\Gamma_n(\mathbf{X}) = 0,$$

$$(2.5) \quad \int_{\Gamma_n} \mathbf{p}(\mathbf{X}) \times \mathbf{t}^n(\mathbf{X})d\Gamma_n(\mathbf{X}) = 0.$$

It should be pointed out that the interaction forces  $\mathbf{t}^n$  together with displacement vectors  $\mathbf{d}$  and  $\mathbf{w}$  are unknowns of the problem which should be determined for each rigid inclusion.

The boundary integral equation (2.2) is applied for all collocation points. Similarly, displacement equations (2.3) and equilibrium equations (2.4) and (2.5) must be formulated for all inclusions, in order to obtain the complete set of equations. The numerical BEM equations are obtained after discretisation of these equations.

The outer boundary of the body and the surfaces of the rigid inclusions are divided into boundary elements as shown in Fig. 2. In the developed computer code eight-node quadratic elements are used.

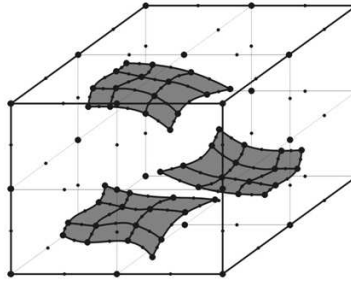


FIG. 2. Discretisation of the body using quadratic boundary elements.

Along the external boundary the variations of coordinates, displacements and tractions are interpolated using quadratic shape functions. Along the surfaces of the inclusions only the variations of coordinates and tractions (interaction forces) are interpolated. The collocation nodes are both the nodes on the external boundary of the body and along the surfaces of the inclusions.

Using Eq. (2.3), the nodal displacement vector  $\mathbf{u}^n$  for an inclusion  $n$  can be related to the rigid-body translation  $\mathbf{d}$  and rotation  $\mathbf{w}$  of that inclusion by the following expression:

$$(2.6) \quad \mathbf{u}^n = \mathbf{A}^n \mathbf{u}_r^n,$$

where  $\mathbf{A}^n$  is the transformation matrix for all nodes of an inclusion and  $\mathbf{u}_r^n$  is the rigid-body displacement vector for an inclusion  $n$ .

The equilibrium equations (2.4) and (2.5) for an inclusion  $n$  can be written in the form:

$$(2.7) \quad \mathbf{B}^n \mathbf{t}_r^n = \mathbf{0},$$

where  $\mathbf{t}_r^n$  is a nodal traction vector for an inclusion  $n$ ,  $\mathbf{B}^n$  is a coefficient matrix for all nodes of an inclusion  $n$  obtained from the equilibrium equations of forces and moments and it depends on the position of inclusion nodes.

Applying Eq. (2.2) for the collocation nodes both along the external boundary and internal surfaces, the following system of numerical equations in the matrix

form is obtained:

$$(2.8) \quad \begin{bmatrix} \mathbf{H}_{ee} & \mathbf{0} \\ \mathbf{H}_{ie} & \mathbf{I} \end{bmatrix} \begin{bmatrix} \mathbf{u}_e \\ \mathbf{u}_i \end{bmatrix} = \begin{bmatrix} \mathbf{G}_{ee} & \mathbf{G}_{ei} \\ \mathbf{G}_{ie} & \mathbf{G}_{ii} \end{bmatrix} \begin{bmatrix} \mathbf{t}_e \\ \mathbf{t}_i \end{bmatrix},$$

where the submatrices with the subscripts **e** and **i** are related to the external boundary and internal surfaces, respectively,  $\mathbf{u}_e$  are displacements of the matrix along the outer boundary,  $\mathbf{u}_i$  are displacements of the matrix along the rigid inclusions,  $\mathbf{t}_e$  are tractions on the outer boundary,  $\mathbf{t}_i$  are tractions acting on the matrix along the inclusions, the submatrices **H** and **G** depend on fundamental solutions and shape functions, and **I** is a unity matrix.

Along the interface between the matrix and the reinforcement, the following conditions of compatibility of displacements and equilibrium of tractions should be satisfied, respectively:

$$(2.9) \quad \mathbf{u}_i = \mathbf{u},$$

$$(2.10) \quad \mathbf{t}_i = -\mathbf{t}_r,$$

where  $\mathbf{u}$  are displacements of the rigid inclusions defined by Eq. (2.6) and formulated for all  $N$  inclusions,  $t_r$  are tractions acting on all inclusions.

Supplying Eq. (2.8) with Equations (2.6) and (2.7) for all inclusions and taking into account the conditions (2.9) and (2.10), the following system of equations is obtained:

$$(2.11) \quad \begin{bmatrix} \mathbf{H}_{ee} & \mathbf{0} \\ \mathbf{H}_{ie} & \mathbf{A} \\ \mathbf{0} & \mathbf{0} \end{bmatrix} \begin{bmatrix} \mathbf{u}_e \\ \mathbf{u}_r \end{bmatrix} = \begin{bmatrix} \mathbf{G}_{ee} & -\mathbf{G}_{ei} \\ \mathbf{G}_{ie} & -\mathbf{G}_{ii} \\ \mathbf{0} & \mathbf{B} \end{bmatrix} \begin{bmatrix} \mathbf{t}_e \\ \mathbf{t}_r \end{bmatrix}.$$

Next, the system of algebraic equations is rearranged in such a way that all the unknown quantities are on the left side and the known quantities on the right side of the equation. The first modification refers to the unknown interaction forces  $\mathbf{t}_r$  and it results in

$$(2.12) \quad \begin{bmatrix} \mathbf{H}_{ee} & \mathbf{G}_{ei} & \mathbf{0} \\ \mathbf{H}_{ie} & \mathbf{G}_{ii} & \mathbf{A} \\ \mathbf{0} & \mathbf{B} & \mathbf{0} \end{bmatrix} \begin{bmatrix} \mathbf{u}_e \\ \mathbf{t}_r \\ \mathbf{u}_r \end{bmatrix} = \begin{bmatrix} \mathbf{G}_{ee} \\ \mathbf{G}_{ie} \\ \mathbf{0} \end{bmatrix} [\mathbf{t}_e].$$

By applying known boundary conditions, the equations are again rearranged and solved. The unknowns are displacements  $\mathbf{u}_e$  and/or tractions  $\mathbf{t}_e$  on the external boundary, rigid-body motions  $\mathbf{u}_r^n$  and tractions  $\mathbf{t}_r^n$  of all  $N$  inclusions.

### 3. Elasto-plastic material

The relation between the mechanical fields can be obtained using the displacement integral equation. For the initial stress approach, the equation has

the form [22]:

$$(3.1) \quad c_{ij}(\mathbf{x}')u_j(\mathbf{x}') = \int_{\Gamma} U_{ij}(\mathbf{x}', \mathbf{x})t_j(\mathbf{x})d\Gamma(\mathbf{x}) - \int_{\Gamma} T_{ij}(\mathbf{x}', \mathbf{x})u_j(\mathbf{x})d\Gamma(\mathbf{x}) \\ + \int_{\Omega} E_{jki}(\mathbf{x}', \mathbf{X})\sigma_{jk}^p(\mathbf{X})d\Omega(\mathbf{X}),$$

where  $E_{jki}$  is a fundamental solution of elastostatics [22] and  $\sigma_{jk}^p$  is the plastic stress, which is the difference between the stresses for the linear-elastic and the elasto-plastic material.

Contrary to the elastostatic case, Eq. (3.1) contains the domain plastic term which depends on the unknown plastic stress  $\sigma_{jk}^p$ . In order to obtain the stress fields in the domain the stress integral equation is used. For the initial stress approach the equation is

$$(3.2) \quad \sigma_{ij}(\mathbf{x}') = \int_{\Gamma} U_{ijk}(\mathbf{x}', \mathbf{x})t_k(\mathbf{x})d\Gamma(\mathbf{x}) - \int_{\Gamma} T_{ijk}(\mathbf{x}', \mathbf{x})u_k(\mathbf{x})d\Gamma(\mathbf{x}) \\ + \int_{\Omega} E_{ijkl}(\mathbf{x}', \mathbf{X})\sigma_{kl}^p(\mathbf{X})d\Omega(\mathbf{X}) + F_{ijkl}^{\sigma}kl^p(\mathbf{x}'),$$

where  $U_{ijk}$ ,  $T_{ijk}$ ,  $E_{ijkl}$  and  $F_{ijkl}^{\sigma}$  are other fundamental solutions [22].

In order to obtain the numerical solution, the boundary is divided into three-node boundary elements and the part of the body where the inelastic behaviour is expected is discretised into eight-node quadrilateral cells, as shown in Fig. 3. The domain discretisation is consistent with the boundary discretisation, i.e., one quadratic cell adjoins one quadratic boundary element. The method requires discretisation of this part of the domain  $\Omega_p$ , which is in the plastic state. The approach requires the plastic domain discretisation, but this procedure does not increase the number of degrees of freedom. The number of equations is equal to the number of degrees of freedom of boundary nodes. The boundary coordinates, displacements, tractions and the stresses in the domain are interpolated by using quadratic shape functions.

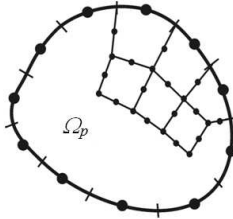


FIG. 3. Discretisation of the body by using quadratic boundary elements and cells.

The displacement integral equation (3.1) is applied to each boundary node. The resulting system of equations can be written in the matrix form as

$$(3.3) \quad \mathbf{H}\mathbf{u} = \mathbf{G}\mathbf{t} + \mathbf{E}\boldsymbol{\sigma}^p,$$

where  $\mathbf{H}$  and  $\mathbf{G}$  depend on boundary integrals of the fundamental solutions  $T_{ij}$  and  $U_{ij}$ , respectively, and boundary shape functions,  $\mathbf{E}$  is dependent on the fundamental solution  $E_{jki}$  and domain shape functions, and  $\boldsymbol{\sigma}^p$  contains components of plastic stress tensor.

The stress integral equations (3.2) are used to determine stresses at all internal nodes of cells. These equations can be written in the matrix form as

$$(3.4) \quad \boldsymbol{\sigma} = \mathbf{G}'\mathbf{t} - \mathbf{H}'\mathbf{u} + \mathbf{E}'\boldsymbol{\sigma}^p,$$

where  $\boldsymbol{\sigma}$  contains components of the stress tensor at all internal nodes of cells. The matrices  $\mathbf{G}'$ ,  $\mathbf{H}'$  and  $\mathbf{E}'$  are obtained similarly as matrices in Eq. (3.3). They depend on appropriate fundamental solutions in Eq. (3.2). The stresses in nodes of the cells at the boundary are computed using boundary tractions and displacements.

The system of equations is modified according to boundary conditions and solved giving unknown boundary quantities and internal stresses. Composite materials are modelled by using the subregion technique. The equations for subregions are assembled using conditions of compatibility of displacements and equilibrium of tractions along common boundaries.

The displacement equation and stress equation contain a vector of not known a priori inelastic stresses  $\boldsymbol{\sigma}^p$ . In order to determine the stresses the load is gradually increased and an iterative procedure is used for each load level to fulfill integral equations [22].

#### 4. Magnetoelastic material

In a Cartesian coordinate system, the  $x_3$  – axis is the poling direction and the  $x_1$ – $x_3$  plane is considered; hence, the generalised plane strain constitutive equations for a magnetoelastic material can be expressed by [21]

$$(4.1) \quad \begin{bmatrix} \sigma_{11} \\ \sigma_{33} \\ \sigma_{13} \\ D_1 \\ D_3 \\ B_1 \\ B_3 \end{bmatrix} = \begin{bmatrix} c_{11} & c_{13} & 0 & 0 & -e_{31} & 0 & -q_{31} \\ c_{13} & c_{33} & 0 & 0 & -e_{33} & 0 & -q_{33} \\ 0 & 0 & c_{44} & -e_{15} & 0 & -q_{15} & 0 \\ 0 & 0 & e_{15} & \kappa_{11} & 0 & a_{11} & 0 \\ e_{31} & e_{33} & 0 & 0 & \kappa_{33} & 0 & a_{33} \\ 0 & 0 & q_{15} & a_{11} & 0 & \mu_{11} & 0 \\ q_{31} & q_{33} & 0 & 0 & a_{33} & 0 & \mu_{33} \end{bmatrix} \begin{bmatrix} \varepsilon_{11} \\ \varepsilon_{33} \\ 2\varepsilon_{13} \\ E_1 \\ E_3 \\ H_1 \\ H_3 \end{bmatrix},$$

where  $\sigma_{ij}$  are components of the stress tensor,  $D_i$  and  $B_i$  denote components of the electric displacement and the magnetic induction vector, respectively,  $\varepsilon_{ij}$  are components of the strain tensor,  $E_i$  and  $H_i$  denote components of the electric and magnetic field vector, respectively. The physical properties of the magnetoelastic material are described by the following tensors:  $c_{ij}$ ,  $\kappa_{ij}$  and  $\mu_{ij}$  are the elastic stiffness, the dielectric and magnetic permeability (permittivity) tensor components;  $e_{ij}$  and  $q_{ij}$  are components of the piezoelectric and piezomagnetic moduli tensors. The electric and magnetic fields are coupled through the magnetoelectric moduli tensor and its components are denoted by the  $a_{ij}$ .

To simplify the notation of equations, generalised quantities can be introduced [15, 23]. By using the generalised quantities one can obtain the generalised Somigliana identity in the form of the boundary integral equations which are analogous to (2.1)

$$(4.2) \quad c_{ij}u_j(\mathbf{x}') + \int_{\Gamma} T_{ij}(\mathbf{x}', \mathbf{x})u_j(\mathbf{x})d\Gamma(\mathbf{x}) = \int_{\Gamma} U_{ij}(\mathbf{x}', \mathbf{x})t_j(\mathbf{x})d\Gamma(\mathbf{x}).$$

In (4.2), the generalised quantities, e.g., the generalised displacement vector  $\mathbf{u}$ , contain both the mechanical and electromagnetic components [15]. The generalised body force vector is neglected in (4.2).

Since the magnetoelastic materials are anisotropic, the fundamental solutions  $T_{ij}(\mathbf{x}', \mathbf{x})$  and  $U_{ij}(\mathbf{x}', \mathbf{x})$  are rather complicated, even for the transversely isotropic model of the material. To obtain the fundamental solutions, the Stroh formalism is used [15]. The Stroh formalism is a powerful and elegant analytic technique for the anisotropic elasticity, which is expanded to the linear magnetoelasticity in this case [24].

Consider a magnetoelastic composite in which the inhomogeneities or voids are in cylindrical shapes, which allows the use of a two-dimensional model of the unit cell as shown in Fig. 4.

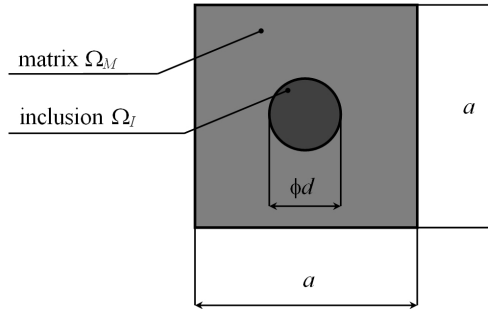


FIG. 4. The unit cell of the magnetoelastic composite.

Let the unit cell shown in Fig. 4 be composed of two parts, which occupy the subdomains  $\Omega_M$  (the matrix) and  $\Omega_I$  (the inhomogeneity). The BEM equations for each subregion have a form [15]:

$$(4.3) \quad \Omega_M : \begin{bmatrix} \mathbf{H}_{MM}^M & \mathbf{H}_{MI}^M \\ \mathbf{H}_{IM}^M & \mathbf{H}_{II}^M \end{bmatrix} \begin{bmatrix} \mathbf{u}_M^M \\ \mathbf{u}_I^M \end{bmatrix} = \begin{bmatrix} \mathbf{G}_{MM}^M & \mathbf{G}_{MI}^M \\ \mathbf{G}_{IM}^M & \mathbf{G}_{II}^M \end{bmatrix} \begin{bmatrix} \mathbf{t}_M^M \\ \mathbf{t}_I^M \end{bmatrix}$$

$$\Omega_I : \mathbf{H}^I \mathbf{u}^I = \mathbf{G}^I \mathbf{t}^I.$$

In Eqs. (4.3)  $\mathbf{H}_{ij}^k$ ,  $\mathbf{G}_{ij}^k$ ,  $\mathbf{u}_i^k$  and  $\mathbf{t}_i^k$  denote the corresponding parts of the  $\mathbf{H}$  and  $\mathbf{G}$  BEM matrices and corresponding parts of the vectors  $\mathbf{u}$  and  $\mathbf{t}$  (which contain the generalised displacements and tractions, respectively) related to the matrix ( $M$ ) or inclusion ( $I$ ) subregion of the unit cell. The superscripts ( $k = M$  or  $I$ ) denote that the submatrix, the subvector, the matrix or the vector are related to the composite matrix or the inclusion subregion, respectively.

To obtain the final set of equations, the interface compatibility and equilibrium equations, must be implemented [15, 21]:

$$(4.4) \quad \begin{aligned} \mathbf{u}_I^M &= \mathbf{u}^I, \\ \mathbf{t}_I^M &= -\mathbf{t}^I. \end{aligned}$$

Equations (4.4) describe the perfect magnetoelctromechanical bonding. Multiplying both sides of (4.3) by the inverse of  $\mathbf{G}$  and implementing (4.4) one can obtain the final system of equations for the generalised displacements [15]:

$$(4.5) \quad \begin{bmatrix} \mathbf{A}_{MM}^M & \mathbf{A}_{MI}^M \\ \mathbf{A}_{IM}^M & \mathbf{A}_{II}^M + \mathbf{A}^I \end{bmatrix} \begin{bmatrix} \mathbf{u}_M^M \\ \mathbf{u}^I \end{bmatrix} = \begin{bmatrix} \mathbf{t}_M^M \\ \mathbf{O}^I \end{bmatrix},$$

where the submatrices  $\mathbf{A} \equiv (\mathbf{G}^{-1}\mathbf{H})$ ,  $\mathbf{O}^I$  is a null matrix of the appropriate dimensions. To solve the system (4.5) it can be rearranged using the prescribed boundary conditions.

## 5. Numerical examples

### 5.1. Material reinforced by a planar rigid-surface inclusion

A three-dimensional unit cell consisting of a single square planar rigid-surface inclusion embedded in an elastic body is considered. The material can be a model of a composite in which a soft matrix is reinforced by very stiff flake-like inclusions. The cube is subjected to the uniform horizontal loading  $q_1$  or to the vertical loading  $q_2$ , as shown in Fig. 5.

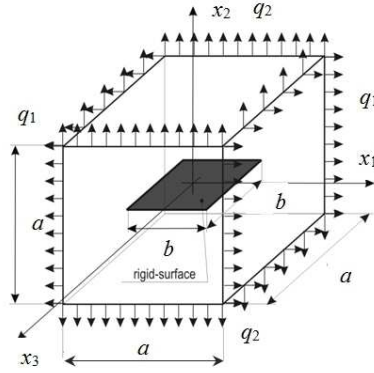


FIG. 5. Unit cell consisting of a rigid inclusion.

The prescribed tractions to the walls of the unit cell are  $q = 1$  MPa. The side length of the unit cell and the inclusion are  $a$  and  $b$ , respectively. A zero-thickness of the inclusion is assumed in the present study. The inclusion is located in the centre of the model along one of its symmetry planes. The material of the cube is isotropic, linearly elastic and has the Poisson ratio  $\nu = 0.3$  and the Young modulus  $E_m = 1$  GPa.

The outer boundary of the 3D cube is divided into 96 quadratic eight-noded boundary elements and the rigid-surface inclusion into 16 quadratic elements. It results in 870 degrees of freedom for the outer boundary plus six rigid-body motions which define displacements of the inclusion.

The computed displacements of external surfaces of the unit cell are used to calculate average strains in the directions of the coordinate system. These strains are used to determine effective Poisson's ratios and the applied tractions and average strains to compute the overall effective Young's moduli [3].

The relative effective Young modulus  $E_{11}/E_m$  and  $E_{22}/E_m$  is computed for different ratios  $b/a$ , where  $E_{11}$  and  $E_{22}$  are the longitudinal and transverse Young modulus of the composite, respectively. Poisson's ratios  $\nu_{ij}$ , which correspond to strains in the  $j$  direction when the load is applied in the  $i$  direction, are also determined. The results are presented in Table 1.

**Table 1. Effective properties of the composite with rigid inclusions.**

Horizontal load $q_1$				Vertical load $q_2$			
$b/a$	0.125	0.250	0.375	$b/a$	0.125	0.250	0.375
$E_{11}/E_m$	1.010	1.075	1.236	$E_{22}/E_m$	1.002	1.014	1.041
$\nu_{12}$	0.301	0.305	0.314	$\nu_{21}$	0.298	0.288	0.265
$\nu_{13}$	0.298	0.288	0.266	$\nu_{23}$	0.298	0.288	0.265

## 5.2. Elasto-plastic material with inclusions

A square representative volume element shown in Fig. 6 contains nine circular inclusions. The length of the edges of the element is  $l = 3$  mm, the distance between centres of the inclusions is  $a = 1$  mm and their diameter is  $d$  (Fig. 6a). Three different diameters of inclusions are considered  $d = 0.3, 0.5, 0.7$  mm. The RVE is subjected to tensile  $q_1$  or shear loading  $q_2$ , as shown in Figs. 6b and 6c, respectively.

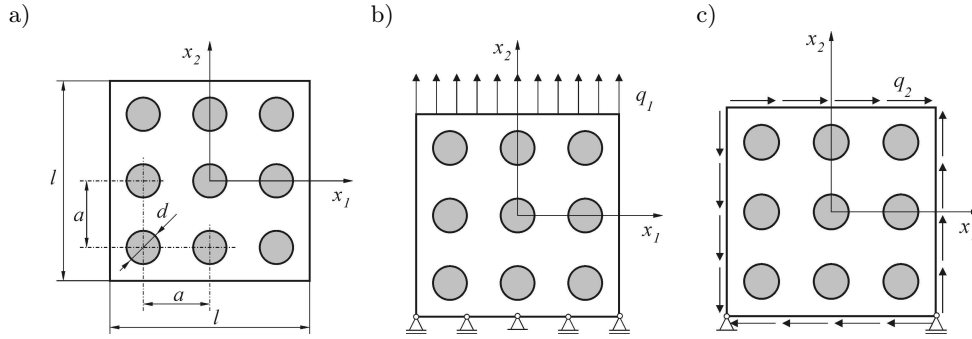


FIG. 6. Representative volume element: a) dimensions, b) tensile loading, c) shear loading.

The displacements of nodes on the external boundary of the RVE are used to compute average strains. The RVE is analysed using the BEM and the FEM. The external boundaries of the RVE are divided into 60 quadratic boundary elements and each inclusion into 10 boundary elements. The materials of the matrix and inclusions are homogeneous and isotropic. The elasto-plastic material with linear isotropic hardening satisfies the Huber–Hencky–von Mises yield criterion. The material properties of the matrix are: the Young modulus  $E = 100\,000$  MPa, the tangent modulus  $H = 25\,000$  MPa, the yield stress  $\sigma_Y = 150$  MPa and the Poisson ratio  $\nu = 0.3$ . The material properties of the inclusion are: the Young modulus  $E = 200\,000$  MPa, the tangent modulus  $H = 50\,000$  MPa, the yield stress  $\sigma_Y = 300$  MPa and the Poisson ratio  $\nu = 0.3$ . The plate is in plane stress state. The relation between applied stress and average strain for tensile and shear loading is shown in Fig. 7. The results computed by the BEM and the FEM agree very well.

The linear parts of the plots are approximated for the material in the elastic and plastic state and used to compute the effective yield stresses and the effective tangent moduli. The effective yield stress is the stress, which corresponds to the point of intersection of lines for the material in the elastic and plastic state. The effective properties for the material subjected to tensile and shear loading are shown in Tables 2 and 3.

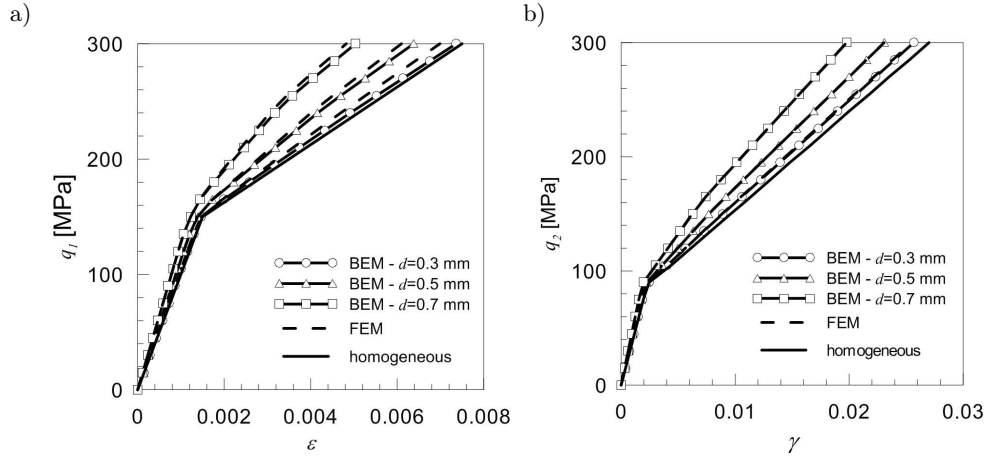


FIG. 7. Applied stress vs. average strain for the RVE with inclusions: a) tensile loading  $q_1$ , b) shear loading  $q_2$ .

Table 2. Effective yield stress of the material [MPa].

Diameter, $d$ [mm]	Tension	Shear
0.0	150	85
0.3	154	90
0.5	168	96
0.7	186	108

Table 3. Effective tangent modulus of the material [MPa].

Diameter, $d$ [mm]	Tension	Shear
0.0	25 000	8600
0.3	24 600	8900
0.5	26 900	9700
0.7	31 800	10 900

### 5.3. Piezoelectromagnetic composite

The most important physical constant, which describes the coupling effect, is the piezoelectric, piezomagnetic or magnetoelectric modulus [25]. In the next numerical example, the  $\text{CoFe}_2\text{O}_4$  piezomagnetic matrix with the  $\text{BaTiO}_3$  piezoelectric inclusion is considered, as shown in Table 4 [24]. Results are obtained using the Mori–Tanaka method and a unit cell shown in Fig. 4 with the volume fraction of inclusions varied from 0 to 0.6. The total mesh size is equal to

52 boundary elements: 40 constant elements for the unit cell external boundary and 12 constant boundary elements for the inclusion boundary. To determine overall properties of the composite the uniform generalised strain, namely the uniform strain and the uniform electric and magnetic field boundary conditions can be applied on the boundary of the unit cell [15]. Next, the Mori–Tanaka numerical homogenisation method is applied [15, 21]. The BEM is applied to calculate the dilute generalised strain concentration tensor.

**Table 4. Material constants for CoFe<sub>2</sub>O<sub>4</sub>/BaTiO<sub>3</sub> composite.**

Material		Matrix CoFe <sub>2</sub> O <sub>4</sub>	Inclusion BaTiO <sub>3</sub>
elastic constants [GPa]	c <sub>11</sub>	286.0	166
	c <sub>13</sub>	170.5	78
	c <sub>33</sub>	269.5	162
	c <sub>44</sub>	45.3	43
piezoelectric moduli [C/m <sup>2</sup> ]	e <sub>51</sub>	0	11.6
	e <sub>31</sub>	0	−4.4
	e <sub>33</sub>	0	18.6
dielectric permittivity [nF/m]	κ <sub>11</sub>	0.080	11.2
	κ <sub>33</sub>	0.093	12.6
magnetic permittivity [μH/m]	μ <sub>11</sub>	−590	5
	μ <sub>33</sub>	157	10
piezomagnetic moduli [N/Am]	q <sub>51</sub>	550.0	0
	q <sub>31</sub>	580.3	0
	q <sub>33</sub>	699.7	0
magnetoelectric moduli [Ns/VC]	a <sub>11</sub>	0	0
	a <sub>33</sub>	0	0

Figure 8 shows the results of the composite magnetic permittivity. As can be seen,  $\mu_{11}^*$  and  $\mu_{33}^*$  tend to the values of the piezoelectric phase when the inclusion fraction increases. A different behaviour of the magnetoelectric moduli (Fig. 9) has been found in responding to the change of the inclusion fraction. In this case, non-monotonic volume fraction behaviour of the effective property is observed.

In this case, it is possible to optimise the coupling effects of composites. As mentioned in [24] the magnetoelectric coupling effect is observed in the composite, which does not exist in either the matrix or the inclusion.

Figure 10 shows the results of the effective piezomagnetic moduli; the effective piezomagnetic moduli are decreased when the inclusion volume fraction increases.

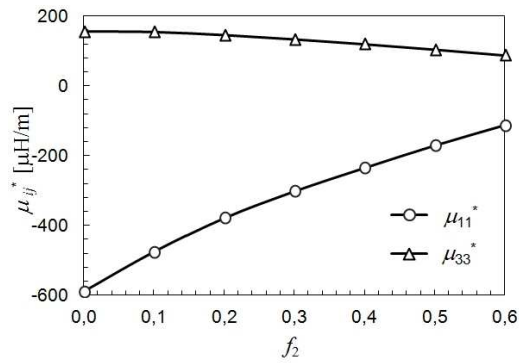


FIG. 8. The effective magnetic permeability  $\mu_{11}^*$  and  $\mu_{33}^*$  vs. inclusion volume fraction  $f_2$  for  $\text{CoFe}_2\text{O}_4/\text{BaTiO}_3$  composite.

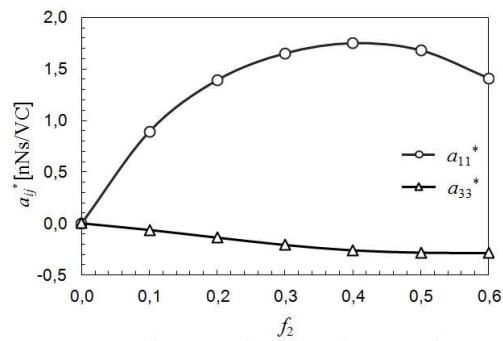


FIG. 9. The effective magnetoelectric moduli  $a_{11}^*$  and  $a_{33}^*$  vs. inclusion volume fraction  $f_2$  for  $\text{CoFe}_2\text{O}_4/\text{BaTiO}_3$  composite.

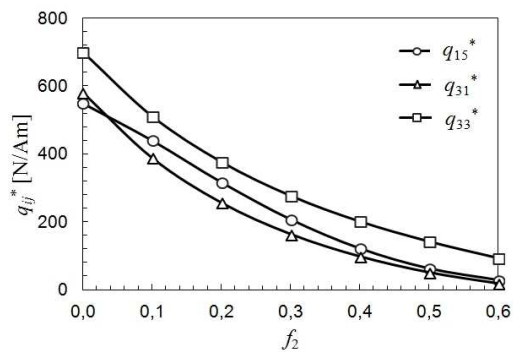


FIG. 10. The effective piezomagnetic moduli  $q_{15}^*$ ,  $q_{31}^*$  and  $q_{33}^*$  vs. inclusion volume fraction  $f_2$  for  $\text{CoFe}_2\text{O}_4/\text{BaTiO}_3$  composite.

## 6. Conclusions

The boundary element method (BEM) is applied to analysis of various microstructures. The influence of volume fractions of inclusions on effective properties of materials is studied by considering a unit cell or a representative volume element. The modelling of such materials is significantly simplified in comparison to domain methods, for example the finite element method (FEM), because nodes are situated only along the external boundary and boundaries of inhomogeneities. Their number, positions, shapes and dimensions can be very simply modified. Knowledge of boundary quantities is sufficient to compute overall properties of microstructures. Additionally, the method gives very accurate results for structures with high stress concentrations, which occur in nonhomogeneous materials. Contrary to analytical methods, solids with high density of constituents can be analysed accurately.

## Acknowledgments

The scientific research was financed by the Ministry of Science and Higher Education of Poland in years 2010–2012.

## References

1. G.W. MILTON, *The Theory of Composites*, Cambridge University Press, Cambridge, 2004.
2. S. NEMAT-NASSER, M. HORI, *Micromechanics: Overall Properties of Heterogeneous Materials*, Elsevier, Amsterdam, 1999.
3. J. QU, M. CHERKAoui, *Fundamentals of Micromechanics of Solids*, John Wiley & Sons, Inc., Hoboken, New Jersey, 2006.
4. M. OSTOJA-STARZEWSKI, *Microstructural Randomness and Scaling in Mechanics of Materials*, Chapman & Hall/CRC Press, Boca Raton-London-New York, 2008.
5. M. KAMIŃSKI, *Boundary element method homogenization of the periodic linear elastic composites*, Engineering Analysis with Boundary Elements, **23**, 815–823, 1999.
6. C.Y. DONG, *The integral equation formulations of an infinite elastic medium containing inclusions, cracks and rigid lines*, Engineering Fracture Mechanics, **75**, 3952–3965, 2008.
7. Y.J. LIU, N. NISHIMURA, Y. OTANI, *Large-scale modeling of carbon-nanotube composites by fast multipole boundary element method*, Computational Materials Science, **34**, 173–187, 2005.
8. Y.J. LIU, N. NISHIMURA, Y. OTANI, T. TAKAHASHI, X.L. CHEN, H. MUNAKATA, *A fast boundary element method for the analysis of fiber-reinforced composites based on a rigid-inclusion model*, Journal of Applied Mechanics, **72**, 115–128, 2005.
9. S. GHOSH, S. MOORTHY, *Elastic-plastic analysis of arbitrary heterogeneous materials with the Voronoi Cell finite element method*, Computer Methods in Applied Mechanics and Engineering, **121**, 373–409, 1995.

10. K. LEE, S. GHOSH, *A microstructure based numerical method for constitutive modeling of composite and porous materials*, Materials Science and Engineering, **A272**, 120–133, 1999.
11. J. LEE, J.G. BOYD, D.C. LAGOUDAS, *Effective properties of three-phase electro-magneto-elastic composites*, International Journal of Engineering Science, **43**, 790–825, 2005.
12. Q.-H. QIN, *Micromechanics-BE solution for properties of piezoelectric materials with defects*, Engineering Analysis with Boundary Elements, **28**, 809–814, 2004.
13. Q.-H. QIN, *Material properties of piezoelectric composites by BEM and homogenization method*, Composite Structures, **66**, 295–299, 2004.
14. H. WANG, G. TAN, S. CEN, Z. YAO, *Numerical determination of effective properties of voided piezoelectric materials using BNM*, Engineering Analysis with Boundary Elements, **29**, 636–646, 2004.
15. P. FEDELIŃSKI [Ed.], *Advanced Computer Modelling in Micromechanics*, Monografia, Nr 427, Wydawnictwo Politechniki Śląskiej, Gliwice, 2013.
16. P. FEDELIŃSKI, R. GÓRSKI, G. DZIATKIEWICZ, J. PTASZNY, *Computer modelling and analysis of effective properties of composites*, Computer Methods in Materials Science, **11**, 3–8, 2011.
17. J. PTASZNY, P. FEDELIŃSKI, *Numerical homogenization of polymer/clay nanocomposites by the boundary element method*, Archives of Mechanics, **63**, 517–532, 2011.
18. R. GÓRSKI, *Elastic properties of composites reinforced by wavy carbon nanotubes*, Mechanics and Control, **30**, 203–212, 2011.
19. P. FEDELIŃSKI, *Computer modeling and analysis of microstructures with fibres and cracks*, Journal of Achievements in Materials and Manufacturing Engineering, **54**, 242–249, 2012.
20. P. FEDELIŃSKI, *Analysis of representative volume elements with random microcracks*, Chapter 17, Computational Modelling and Advanced Simulation, J. MURIN *et al.* [ed.], Computational Methods in Applied Sciences, **24**, Springer Science+Business Media B.V., 333–341, 2011.
21. G. DZIATKIEWICZ, *Analysis of effective properties of piezocomposites by the subregion BEM-Mori-Tanaka approach*, Mechanics and Control, **30**, 194–202, 2011.
22. X.W. GAO, T.G. DAVIES, *Boundary Element Programming in Mechanics*, Cambridge University Press, Cambridge, 2002.
23. E.A. PAN, *BEM analysis of fracture mechanics in 2D anisotropic piezoelectric solids*, Engineering Analysis Boundary Elements, **23**, 67–76, 1999.
24. J.Y. LI, *Magneto-electroelastic multi-inclusion and inhomogeneity problems and their applications in composite materials*, International Journal of Engineering Science, **38**, 1993–2011, 2000.
25. J.J. TELEGA, A. GALKA, B. GAMBIN, *Effective properties of physically nonlinear piezoelectric composites*, Archives of Mechanics, **50**, 321–340, 1998.

Received May 13, 2013; revised version November 27, 2013.